

Computed Tomography Image Reconstruction in 3D VoxelSpace

M.S.M. Yusoff*, R. Sulaiman*, K. Shafinah**, R. Fatihah***

*Institute of Visual Informatics, National University of Malaysia (UKM), 43600 Bangi, Selangor, Malaysia.

**Faculty of Agriculture and Food Sciences, Universiti Putra Malaysia Bintulu Sarawak Campus, Nyabau Road, P.O. Box 396, 97008 Bintulu, Sarawak.

***Faculty of Computer Science and Information Technology, Universiti Malaysia Sarawak (UNIMAS), 94300 Kota Samarahan, Sarawak, Malaysia.

ABSTRACT : The aim of the study was to investigate the relationship between 2D gray scale pixels and 3D gray scale pixels of image reconstructions in computed tomography (CT). The 3D space image reconstruction from data projection was a challenging and difficult research problem. The image was normally reconstructed from the 2D data from CT data projection. In this descriptive study, a synthetic 3D Shepp-Logan phantom was used to simulate the actual data projection from a CT scanner. Real-time data projection of a human abdomen was also included in this study. Additionally, the Graphical User Interface (GUI) for the application was designed using Matlab Graphical User Interface Development Environment (GUIDE). The application was able to reconstruct 2D and 3D images in their respective spaces successfully. The image reconstruction for CT in 3D space was analyzed along with 2D space in order to show their relationships and shared properties for the purpose of constructing these images.

KEYWORDS: - Computed Tomography, DICOM, Image reconstruction, Pixels, Voxels,

I. INTRODUCTION

This research focuses on aspects of image reconstruction for computed tomography (CT) in 3D space. Sinogram images are a raw projection of data from the CT scanner that is plotted to show a graphical view of the projection data. These images were often incomprehensible and useless especially for applications in industrial business or in vitro medicine. Should it be possible to reconstruct these images rigorously through the application of suitable algorithms, then the invaluable hidden properties and information contained within the images of these internal object structures could be displayed as real world images.

The transformation of sinogram data into an ontological cross-section image is often labeled as image reconstruction in computed tomography [1]. Fig. 1 shows a simple illustration of the physical schematics of a CT scanner. They consist of an x-ray source, detector assembly array, radiation collimators and a patient bed conveyor.

They were set-up and aligned to measure the heterogeneous density of x-ray readings after penetrating the object. According to [2] the log-attenuation count was a sinogram or projection data that consists of a multiple 2D cross-section arrangement.

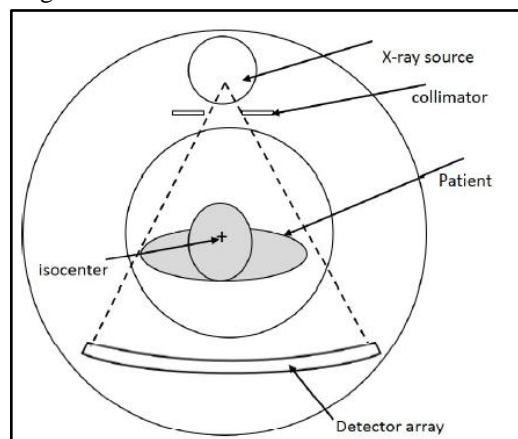


Figure 1: A simple model of a CT scanner [2]

II. RESEARCH METHOD

According to [3] research, the 3D sinograms wererebinding into 2D projections to perform the forward and backprojection operations, but were converted back into 3D sinograms in between each iteration. Also, according to [4], the 3D cone-beam projections of $N \times N \times M$ pixels were decomposed to separate the 2D parallel-beam projections.

The FDK method is a notable algorithm that reconstructs a 3D volume from multiple 2D projections. In this method, each of the 2D projections were weighted, filtered and back-projected, then constructed in a solid 3D form [5]. This optimization method was unavoidable in CT image reconstruction due to the large size of the volumes. It holds millions of voxels and the sinogram may consist of millions of projection measurements [6].

2.1 Radon Transform

The projection problems in CT scans were mathematically explained by the function of Radon transformation[7]. Therefore, many difficult computational methods have been developed to solve the reconstruction problems of the inverse Radon transformation[8].The image reconstruction begins with data collection. This study used the Digital Imaging and Communications in Medicine (DICOM) data format[9]which was created or collected within the study period. In order to create and built a DICOM data, the raw data was initially transformed into a 1D vector and then reshaped into the desired 3D format.

2.2 The pixels and voxels

The standard terms of pixels and voxels are widely used to represent the basic measurements of a picture. Pixels were defined as an element that has two dimensions, the horizontal dimension representing the element's x-axis and the vertical dimension representing the element's y-axis. Concurrently voxels or 3D pixels were defined as having a 3D spatial resolution which were stored in the sequence of x-y-z[10]. Fig. 2 shows the differences between these three types of image space. First, the image in 2D pixels as shown in Fig. 2(a) and Fig. 2 (b), secondly the image in 3D pixels as shown in Fig.2 (c) and Fig. 2(d) and finally, the image in voxels as in Fig. 2(e) and Fig. 2(f).

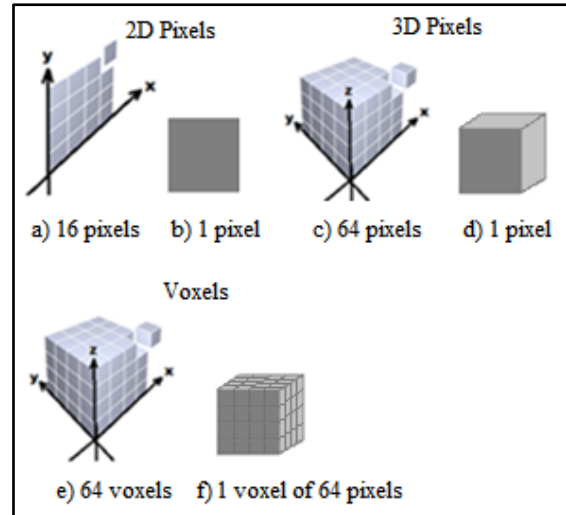


Figure 2: The 2D pixels, 3D pixels and voxels model

Voxels are often illustrated as a solid rectangular model, its dimensions were measured by the reconstruction field-of-view (FOV) and slice thickness [11]

2.3 The basic concept of cross-sectional planes

The human body can be viewed as three sets of cross-sectional universal planes [12]. The first plane is the top view plane, which runs parallel to the ground. It is referred to by several different names such as the transverse plane, horizontal plane, axial plane, transaxial plane or x-z plane. The second plane is the side view plane which is often referred to as the sagittal plane, lateral plane or y-z plane. Finally the third plane known as the front view plane and often referred to as the coronal plane, frontal plane or y-x plane. Fig. 3 shows the diagram of axial, sagittal and coronal cross-section planes of the human body.

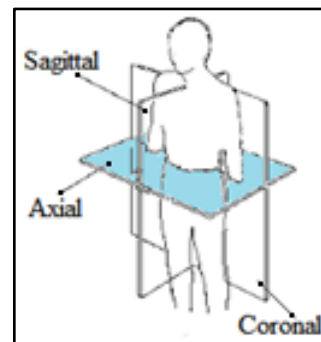


Figure 3: The diagram of axial, sagittal and coronal cross-section planes

2.4 Conceptual of CT Data visualization

In science and engineering, data points are commonly acquired through sampling and experimentation. These function as plots to construct a rough figure. However, through numerical analysis known as the interpolation method, additional data can be generated to plot a smoother graphical image. This is known as curve fitting or regression analysis [13]. Fig. 4 shows the fundamental flow diagram of a 3D image reconstruction [14]. The image interpolation algorithm of the 3D image reconstruction was carried out from original images by adhering to the fundamental flow diagram.

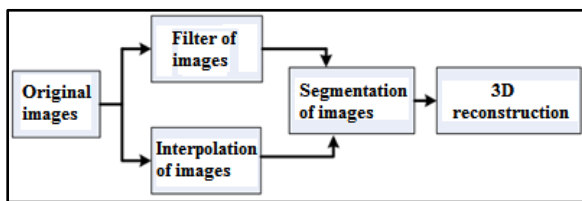


Figure 4: The fundamental flow diagram of 3D image reconstruction [14]

2.5 2D Pixel-Based Method

The pixel building blocks were established from two common parameters, namely the image length and width [15]. Table 1 shows a simple concept of 2D numerical raw data intensity. The table's rows consist of nine pixel elements representing the dimension's length, similarly the table columns consist of nine pixel elements representing the dimension's width. The rows and columns represent a slice in 2D pixels. As for this study, the zero value will be represented using the color the black's density and the one value will be represented by the density of the color white. The zeros can be visualized as a plus sign image from the raw data itself. The raw data can then be saved in a file or stored within the database system for easy retrieval in the future.

Table 1: The raw numerical data represent intensity in 2D

1	1	1	1	0	1	1	1	1
1	1	1	1	0	1	1	1	1
1	1	1	1	0	1	1	1	1
1	1	1	1	0	1	1	1	1
0	0	0	0	0	0	0	0	0
1	1	1	1	0	1	1	1	1

1	1	1	1	0	1	1	1	1
1	1	1	1	0	1	1	1	1
1	1	1	1	0	1	1	1	1

Table 2 shows the addresses location of the pixels' for the 2D pixels from the raw data intensity as shown in Table 1. The location was specifically used to display the corresponding pixel intensity on the computer screen.

Table 2: The addresses of the 2D pixels' location of the raw data intensity as shown in Table 1

(1,1)	(1,2)	(1,3)	(1,4)	...	(1,9)
(2,1)	(2,2)	(2,3)	(2,4)	...	(2,9)
(3,1)	(3,2)	(3,3)	(3,4)	...	(3,9)
(4,1)	(4,2)	(4,3)	(4,4)	...	(4,9)
(5,1)	(5,2)	(5,3)	(5,4)	...	(5,9)
(6,1)	(6,2)	(6,3)	(6,4)	...	(6,9)
(7,1)	(7,2)	(7,3)	(7,4)	...	(7,9)
(8,1)	(8,2)	(8,3)	(8,4)	...	(8,9)
(9,1)	(9,2)	(9,3)	(9,4)	...	(9,9)

Finally, Fig. 5 shows a 2D image that was reconstructed from the data in Table 1 using MATLAB numerical computing language. This 2D image was significant to further the knowledge for the reconstruction of the targeted 3D image used in the present study.

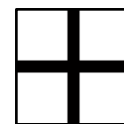


Figure 5: The 2D image constructed from the raw data intensity in Table 1

2.6 3D Pixel Method

In contrast to the 2D pixels, the 3D pixels building blocks were established from three parameters consisting of the length, width and height data. Table 3(a) and (b) shows a concept of the 3D raw numerical data intensity. The rows in the table represent the dimension's length and the columns represent the dimension's width similarly to those of the 2D pixels. Therefore, 3D data consisted of a collection of 2D data. Hence, 3D data blocks required two or more 2D datasets to reconstruct a 3D image. Again, in 3D space, the

value of zero are represented by the intensity of the color black and the value of one was represented by the intensity of the color white.

Table 3: The raw numerical data representing data in 3D space

1	1	1	1	0	1	1	1	1
1	1	1	1	0	1	1	1	1
1	1	1	1	0	1	1	1	1
1	1	1	1	0	1	1	1	1
0	0	0	0	0	0	0	0	0
1	1	1	1	0	1	1	1	1
1	1	1	1	0	1	1	1	1
1	1	1	1	0	1	1	1	1
1	1	1	1	0	1	1	1	1
1	1	1	1	0	1	1	1	1

a) First 2D Slice

b) Second 2D Slice

Table 4 and Table 5 show the 3D pixels address locations from the raw data intensity shown previously in Table 3(a) and (b). The location was specifically used to display the corresponding pixel intensity on the computer screen. As in Table 4 and Table 5, there are three values in each cell of 3D pixels representing each corresponding row, column and depth.

Table 4: The location address of the first slice of the raw data intensity as shown in Table 3(a)

(1,1,1)	(1,2,1)	(1,3,1)	...	(1,9,1)
(2,1,1)	(2,2,1)	(2,3,1)	...	(2,9,1)
(3,1,1)	(3,2,1)	(3,3,1)	...	(3,9,1)
(4,1,1)	(4,2,1)	(4,3,1)	...	(4,9,1)
(5,1,1)	(5,2,1)	(5,3,1)	...	(5,9,1)
(6,1,1)	(6,2,1)	(6,3,1)	...	(6,9,1)
(7,1,1)	(7,2,1)	(7,3,1)	...	(7,9,1)
(8,1,1)	(8,2,1)	(8,3,1)	...	(8,9,1)
(9,1,1)	(9,2,1)	(9,3,1)	...	(9,9,1)

Table 5: The location address of the second slice of the raw data intensity as shown in Table 3(b)

(1,1,2)	(1,2,2)	(1,3,2)	...	(1,9,2)
(2,1,2)	(2,2,2)	(2,3,2)	...	(2,9,2)
(3,1,2)	(3,2,2)	(3,3,2)	...	(3,9,2)
(4,1,2)	(4,2,2)	(4,3,2)	...	(4,9,2)
(5,1,2)	(5,2,2)	(5,3,2)	...	(5,9,2)
(6,1,2)	(6,2,2)	(6,3,2)	...	(6,9,2)
(7,1,2)	(7,2,2)	(7,3,2)	...	(7,9,2)

(8,1,2)	(8,2,2)	(8,3,2)	...	(8,9,2)
(9,1,2)	(9,2,2)	(9,3,2)	...	(9,9,2)

Finally, Fig. 6 shows the image plot using 3D data from Table 3(a) and (b) using MATLAB numerical computing language.

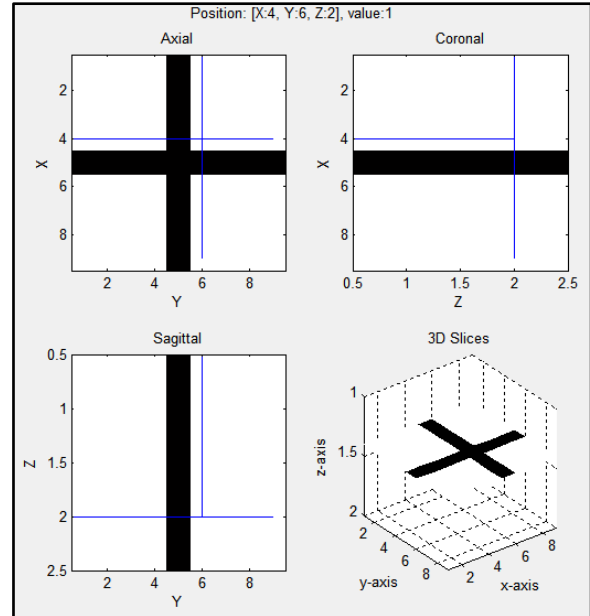


Figure 6: Images of 3D density plot from Table 3(a) and (b)

2.7 Voxel-Based Methods

The voxels were 3D coordinates in spatial space similar to the 3D pixels which were also established from the three basic parameters of length, width and height. The voxel method consists of 3D pixels in the shape of 3D cubes which formed the complete objects. According to [16] each voxel infrastructure can be recognized as a 3D pixel which was similar to the dimensions of a cube. Fig. 7 shows the result of voxels produced through the use of MATLAB add-on application GIBBON created by [17]. The images were reconstructed from a homogeneous intensity data to show a 3D concept through the voxel-based method.

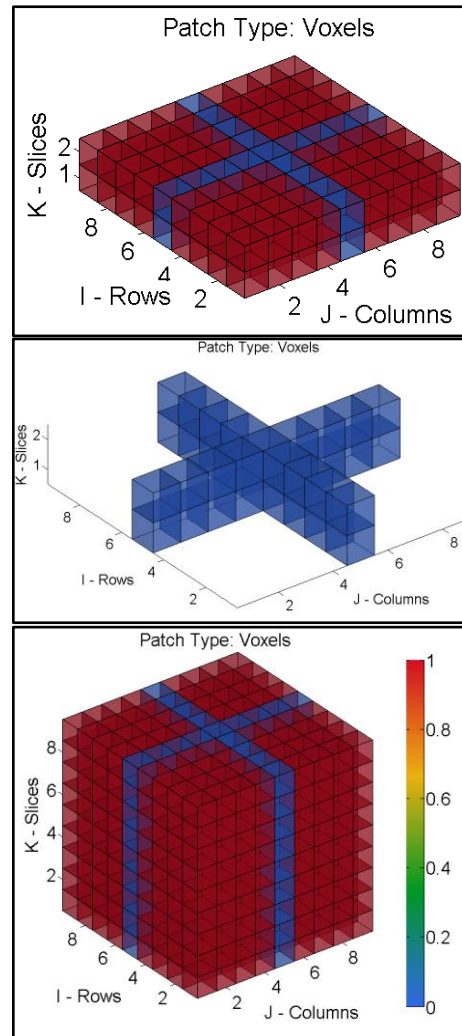
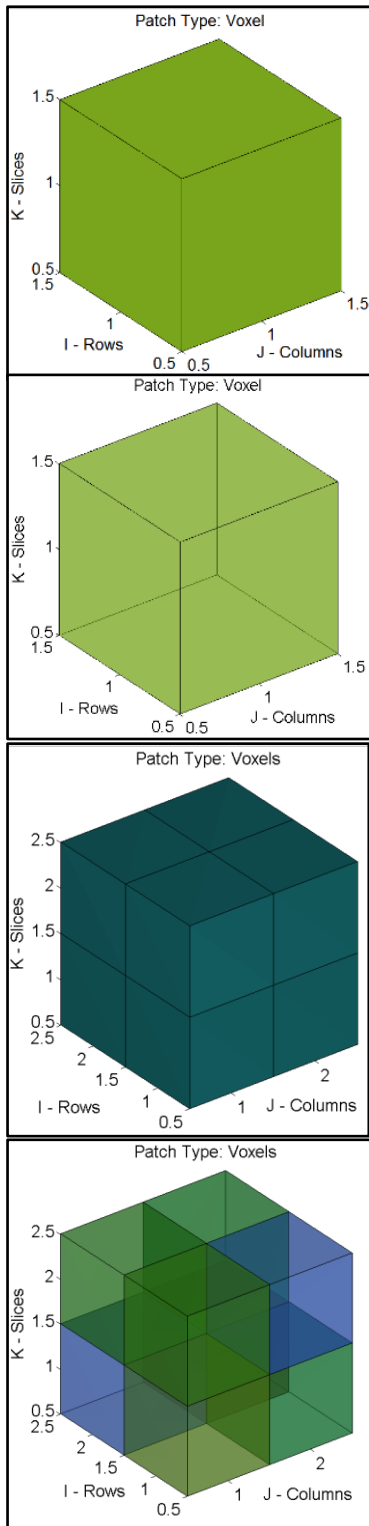


Figure 7: Voxels[17]

The voxel-based method can easily be understood by viewing their appropriate sketches. Figure 8 shows MATLAB dimension cube of the x, y and z dimension from the origin of point (0, 0, 0). This singleton cube is the conceptual building block of a much larger voxel dimension with contrasting intensities.

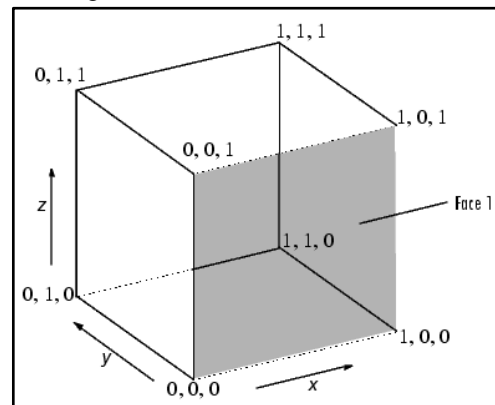


Figure 8: MATLAB dimensional cube

III. RESULTS AND ANALYSIS

The prototype application was developed based on the MATLAB script program and information from previous literature dedicated to 3D image reconstruction of computed tomography. The 3D data projection was obtained from an online research platform (with consent to use obtained for research purposes). Figure 9 shows the axial, coronal and sagittal views of a 3D Shepp-Logan phantom. These images were built with a similar program as those discussed in the methodology section, but with the addition of a 3D phantom in DICOM format. The axial, coronal and sagittal views were changed and corresponded accordingly to the x,y mouse location on a picture canvas. Figure 10 shows the internal properties of a human abdomen from a DICOM data projection in 3D.

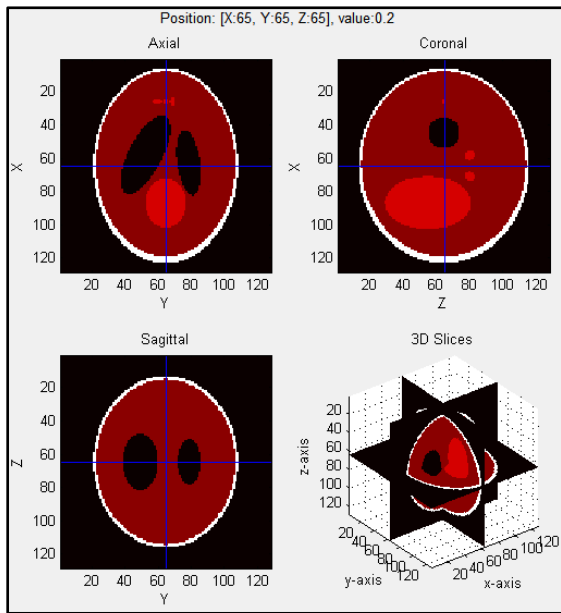


Figure 9: Axial, Coronal and Sagittal Views

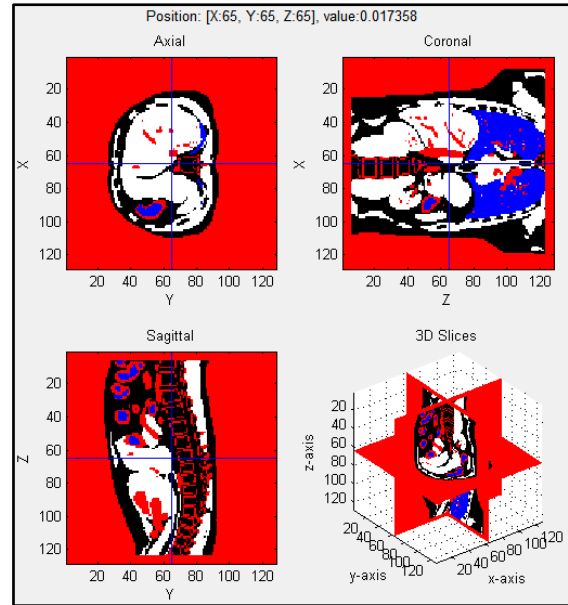


Figure 10: 3D Images Slices of Axial, Coronal and Sagittal

Additionally, Figure 11 shows slices of 2D axial views from a synthetic 3D Shepp-Logan phantom data projection. These slices were displayed using a four times four grid. The images were created using MATLAB script function of phantom3das proposed by Matthias Christian Schabel of the Department of Radiology, University of Utah. There are several free and paid tools running on various platforms with the capability to slice a 3D image into 2D slices, for example 3Dslicer, OsiriX, SliceOmatic and Seg3D.

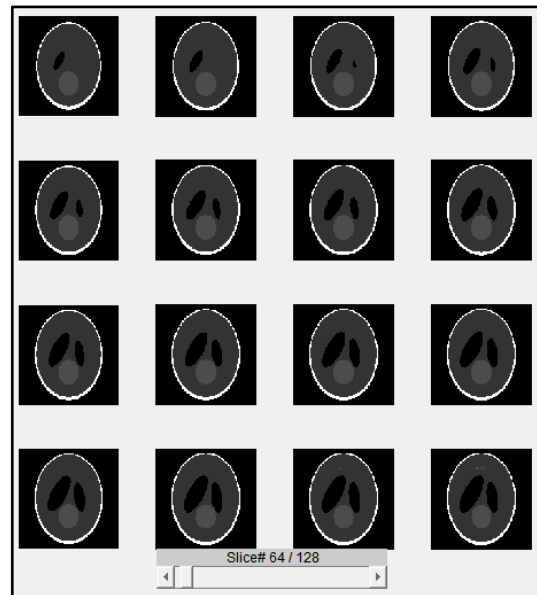


Figure 11: 2D Slices of Axial Views

Fig. 12 shows a 3D voxel-based imageplotted using MATLAB add-on application GIBBON. Fig. 12 a) shows the 3D slicer tool used to slice the object visually in 3D space; while Fig. b) shows a 3D Shepp-Logan phantom image; and last of all, Fig. 12 c) shows a 3D gray scale of a human heart. The slicer can move in the x-axis, y-axis and z-axis to perform the task of slicing.

c) 3D gray scale of a human heart

Figure 12: 3D views a) 3D slicer tool b) 3D phantom image c) 3D gray scale of a human heart

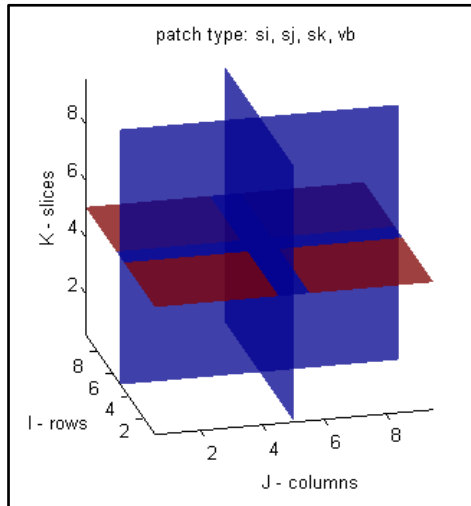
The experiments in the present study were conducted on computers running the Windows 7 and Windows 10 operating system with a minimum hardware requirement of Intel Core i5-2410M, CPU (2.3GHz), 4GB DDR3 RAM and 750 GB HDD. The major application software utilized for the purposes of the study was Matlab version 2008a with image functionality capabilities.

IV. CONCLUSION

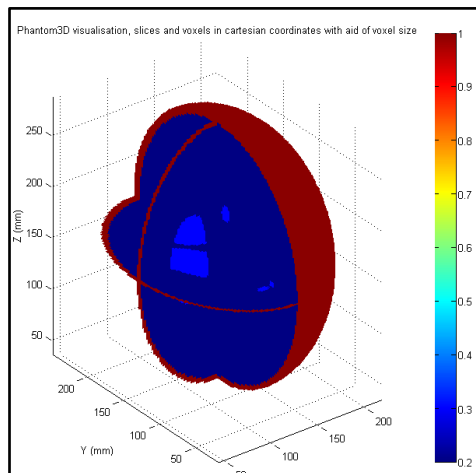
The image reconstruction for CT in 3D space was studied along with 2D space to show the shared properties they hold to build an image. The 3D images could be used to represent a real image that will help people to recognize the scan's object without requiring a detailed description.

REFERENCES

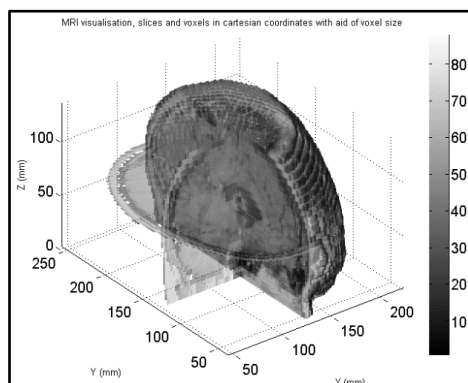
- [1] Quinto, E. T. An Introduction to X-ray tomography and Radon Transforms. In *Proceedings of the Proceedings of Symposia in Applied Mathematics The Radon Transform, Inverse Problems, and Tomography*. American Mathematical Society, Atlanta, 2006, 1-23.
- [2] Karimi, S. *Metal Artifact Reduction in Computed Tomography*. Ph.D., University of California, San Diego, Ann Arbor, 2014.
- [3] Keesing, D. B. *Development and Implementation of Fully 3D Statistical Image Reconstruction Algorithms for Helical CT and Half-Ring PET Insert System*. Dissertation, Washington University, All Theses and Dissertations (ETDs), 2009.
- [4] George, A. K. *Algorithms for tomographic reconstruction: Fast backprojection and cardiac computed tomography* University of Illinois Urbana, Illinois 2007.
- [5] Leeser, M., Mukherjee, S. and Brock, J. Fast reconstruction of 3D volumes from 2D



a) 3D slicer tool



b) 3D phantom image



- CT projection data with GPUs. *BMC Research Notes*, 7(1), 2014, 1-8.
- [6] Jørgensen, J. S. H., Per Christian; Schmidt, Søren *Sparse Image Reconstruction in Computed Tomography*. PhD, Technical University of Denmark, 2013.
- [7] Clackdoyle, R. and Noo, F. A large class of inversion formulae for the 2D Radon transform of functions of compact support. *Inverse Problems*, 20(4), 2004, 1281-1291.
- [8] Gottlieb, D., Gustafsson, B. and Forssen, P. On the direct Fourier method for computer tomography. *Medical Imaging, IEEE Transactions on*, 19(3), 2000, 223-232.
- [9] Flanders, A. E. and Carrino, J. A. Understanding DICOM and IHE. *Seminars in Roentgenology*, 38(3), 2003, 270-281.
- [10] Mueller, K. *Fast and Accurate three-dimensional reconstruction from cone-beam projection data using algebraic methods*. PhD, The Ohio State University, 1998.
- [11] Hsieh, J., Nett, B., Yu, Z., Sauer, K., Thibault, J.-B. and Bouman, C. A. Recent Advances in CT Image Reconstruction. *Current Radiology Reports*, 1(1), 2013, 39-51.
- [12] Ohnesorge, B. M., Flohr, T. G., Becker, C. R., Knez, A. and Reiser, M. F. *Multi-slice and Dual-source CT in Cardiac Imaging* (Springer Berlin Heidelberg, 2007).
- [13] Xu, J. *Data Interpolations*. Apress, 2010.
- [14] Xueli, Z., Wanggen, W., Zhenghua, Z., Rui, W. and Feng, Q. A novel interpolation algorithm for 3D reconstruction of medical images. In *Proceedings of the Audio Language and Image Processing (ICALIP), 2010 International Conference*, 2010, 797-801.
- [15] Smith, S. and Ray, A. *A Pixel Is Not A Little Square, A Pixel Is Not A Little Square, A Pixel Is Not A Little Square!* (And a Voxel Is Not A Cube)". Microsoft Technical Memo 6. Microsoft. 1995.
- [16] Chan, L. H. *Synthetic three-dimensional voxel-based microstructures that contain annealing twins*. Ph.D., Carnegie Mellon University, Ann Arbor, 2010.
- [17] Moerman, K. M. *GIBBON (Hylobates Lar)*. Zenodo, 2016.